COMPUTER METHODS IN APPLIED MECHANICS AND ENGINEERING 76 (1989) 17–40
NORTH-HOLLAND

A FINITE ELEMENT DYNAMIC ANALYSIS OF SPATIAL MECHANISMS WITH FLEXIBLE LINKS

Ben JONKER*
Faculty of Mechanical Engineering, Delft University of Technology, 2628 CD Delft, The Netherlands

Received 28 June 1988
Revised manuscript received 5 December 1988

A finite element based method is presented for dynamic analysis of spatial mechanisms with flexible links. In this analysis the geometrically nonlinear relations for the element deformations in terms of the nodal position and orientation coordinates play a central role. The equations of motion are formulated in terms of mixed sets of generalized coordinates of the mechanism with rigid links and deformation mode coordinates that characterize deformation of the elements. A dynamic simulation of a spatial slider crank mechanism with flexible connecting rod and a simulation of a rotating shaft passing through the major critical speed is presented.

1. Introduction

Though presently the finite element method is usually put forward as a numerical method for the analysis of the strength and stiffness of complex structures, the method has proved to be also particularly useful in the kinematic and dynamic analysis of mechanisms.

The key point in the finite element theory underlying this analysis is the specification of deformation modes in the description of strain, stress and associated stiffness of the elements. This way of finite element discretization forms the algebraic analogy of the continuous field concept for the description of deformations and stresses of deformable bodies. The deformation mode approach has been originated in the early 1960's by Argyris [1], Besseling [2] and Robinson [3]. The definition of the deformation modes, by Argyris termed natural modes includes the specification of rigid body displacements as displacements for which the deformations are zero. If we define the deformation modes by nonlinear functions of the nodal coordinates, valid for arbitrarily large displacements and rotations, then also mechanisms can be analyzed. The ease, by which the deformability can be handled, leads to interesting possibilities of modelling joint elements like sliders and hinges.

Characteristic for the present finite element approach to mechanism analysis is that both links and joints are considered as specific finite elements. Permanent contact between the elements is obtained by letting them have nodal points in common and in these nodal points they share some or all of the coordinates of these points. Instead of constraint equations in the

* Present address: Twente University of Technology, Faculty of Mechanical Engineering, 7500 AE Enschede, The Netherlands.

0045-7825/89/$3.50

points of contact of the links, as is usual in the multibody description, in the finite element method we have to impose conditions on the deformation modes of the elements. Because of the fact that we start out from expressions for the deformation modes as functions of the nodal coordinates, it is easy to extend the analysis to the case of mechanisms with deformable links. Then constitutive equations for the deformations have to be supplied.

The finite element formulation for mechanisms has been utilized by van der Werff [4, 5] and Jonker [6]. In these publications an algorithm is presented for numerical determination of the geometric transfer functions of multi-degree of freedom mechanisms. These functions describe the configuration and deformation state of the mechanism in terms of the degrees of freedom of the mechanism. The degrees of freedom can be defined using a combination of generalized coordinates of the mechanism with rigid links and flexible deformation mode coordinates describing vibrations of flexible links.

The inertia properties of the elements are described using either the lumped or consistent mass formulation. In the lumped formulation rigid bodies with equivalent mass and rotational inertias are attached to the end nodes of the element. The lumped masses and rotational inertias are calculated by assuming that the elements behave like a rigid body. The inertia properties of flexible elements can be modelled more exactly by consistent mass matrices [7]. The main difficulty arising with the derivation of the consistent mass formulation for flexible beam elements is the nonlinear effect of large rotations, resulting in configuration and velocity dependent inertia matrices for the element involving the flexible deformation mode coordinates and its first time derivatives. When only large rotations need to be considered, and angular rates remain small, the conventional consistent mass matrix is still applicable provided that the mass matrix is transformed to the actual configuration of the element [8]. However, for large angular rates, nonlinear dynamic effects associated with the flexible deformations of the element have to be taken into account, even though these deformations remain small.

By means of the first and second-order geometric transfer functions, the equations of motion are formulated in terms of the degrees of freedom, thereby eliminating the constraint forces associated with the rigid link motion. This approach is based on the principle of virtual power (Jourdain's principle [9]) and leads to a minimal system of ordinary differential equations of motion that can be effectively solved numerically. A general purpose computer programme, called SPACAR, based on the presented theory has been developed [10].

2. Finite elements

One of the basic steps in any finite element dynamic analysis of a mechanism is creating its representation as an assembly of finite elements interconnected by coupling elements such as hinges and prismatic joints. The links may be modelled by one or more beam elements that may be rigid or deformable, depending on whether the flexibility is expected to play a role in the dynamic analysis. A number of beam elements can be used to model a complex-shaped link or to obtain a more accurate analysis of critical links in a mechanism.

The location of each element is specified by a set of nodal coordinates $(x_i^k) \in X^k$, some of which may be Cartesian coordinates (x_i^k) of the end nodes, while others describe the orientation of orthogonal triads, rigidly attached at the element nodes and will be denoted by (λ_i^k). The superscript k is added to show that a specific element k is considered. We call X^k

the configuration space of the element k. With respect to some reference configuration of the element, the instantaneous values of the nodal coordinates represent a fixed number of deformation modes for the element. The number of deformation modes is equal to the number of nodal coordinates minus the number of degrees of freedom of the element as a rigid body. In this way we can define for each element a map

$$\boldsymbol{D}^k : X^k \rightarrow E^k , \quad \text{or } \boldsymbol{e}^k = \boldsymbol{D}^k(\boldsymbol{x}^k) , \tag{2.1}$$

where $\boldsymbol{e}^k$ is the vector of deformation mode coordinates $(e_i^k) \in E^k$, some of which are associated with large relative displacements and rotations (e_i^k) between the element nodes, while others describe small elastic deformations of the element and will be denoted by (ε_i^k). We call E^k the deformation space of the element k. The deformation mode coordinates must be invariant with respect to rigid body motions of the element. This necessarily implies geometrically nonlinear expressions for the deformation mode coordinates as functions of the nodal coordinates. The deformation functions are chosen such that they have a clear physical meaning. This facilitates the description of strength and stiffness. The map $\boldsymbol{D}^k$ and its derivative maps

$$\mathrm{D}_i \boldsymbol{D}^k = \frac{\partial \boldsymbol{D}^k}{\partial x_i^k} \quad \text{and} \quad \mathrm{D}_{ij} \boldsymbol{D}^k = \frac{\partial^2 \boldsymbol{D}^k}{\partial x_i^k \partial x_j^k} ,$$

play a major role in the derivation of the theory. In the next sections explicit expressions are presented for the deformation functions $\boldsymbol{D}^k$ of the spatial beam element and the cylindrical hinge element. With these elements it is possible to describe a large class of spatial mechanisms. For the expressions of the derivative maps $\mathrm{D}\boldsymbol{D}^k$ and $\mathrm{D}^2\boldsymbol{D}^k$ the reader is referred to [6].

2.1. *The spatial beam element*

Figure 1 shows a spatial beam element in an x, y, z inertial coordinate system. The configuration of the element is determined by the position vectors $\boldsymbol{x}^p$ and $\boldsymbol{x}^q$ of the end nodes and the angular orientation of orthogonal triads $(\boldsymbol{n}_{\bar{x}}, \boldsymbol{n}_{\bar{y}}, \boldsymbol{n}_{\bar{z}})$ rigidly attached to each end point. In the undeflected state the triads coincide with the axis pq and the principle axes of its cross section. The rotation part of the motion of the (flexible) beam is described by the rotation of the triads $(\boldsymbol{n}_{\bar{x}}, \boldsymbol{n}_{\bar{y}}, \boldsymbol{n}_{\bar{z}})$ which are determined by rotation matrices $\boldsymbol{R}^p$ and $\boldsymbol{R}^q$. If the beam is rigid then the rotation matrices are identical and in the initial undeflected state they are equal to the identity matrix. The components of the rotation matrices are expressed in terms of Euler parameters [11]. In this case the rotation matrix $\boldsymbol{R}$ can be written in terms of four Euler parameters λ_0, λ_1, λ_2, λ_3 as

$$\boldsymbol{R} = \begin{bmatrix} \lambda_0^2 + \lambda_1^2 - \lambda_2^2 - \lambda_3^2 & 2(\lambda_1\lambda_2 - \lambda_0\lambda_3) & 2(\lambda_1\lambda_3 + \lambda_0\lambda_2) \\ 2(\lambda_1\lambda_2 + \lambda_0\lambda_3) & \lambda_0^2 - \lambda_1^2 + \lambda_2^2 - \lambda_3^2 & 2(\lambda_2\lambda_3 - \lambda_0\lambda_1) \\ 2(\lambda_1\lambda_3 - \lambda_0\lambda_2) & 2(\lambda_2\lambda_3 + \lambda_0\lambda_1) & \lambda_0^2 - \lambda_1^2 - \lambda_2^2 + \lambda_3^2 \end{bmatrix} . \tag{2.2}$$

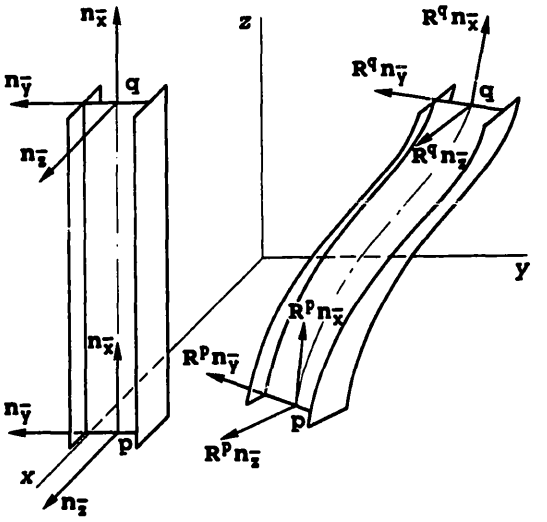

Fig. 1. Beam element, initial and deformed state.

By definition the Euler parameters satisfy the constraint equation

$$\lambda_0^2 + \lambda_1^2 + \lambda_2^2 + \lambda_3^2 = 1\,, \quad \text{or } \boldsymbol{\lambda}^t\boldsymbol{\lambda} = 1\,. \tag{2.3}$$

The use of Euler parameters avoids singularity problems associated with Euler angles, and has the additional advantage that the components of the transformation matrices are quadratic algebraic expressions in terms of these parameters, instead of complicated goniometric functions, as is the case when using Euler angles for instance; algebraic expressions are computationally more efficient than goniometric functions.

With the vector $\boldsymbol{l}^k = \boldsymbol{x}^q - \boldsymbol{x}^p$, the deformation functions of the beam element can now be written as follows [12]:

$$\text{elongation:}\quad \varepsilon_1^k = D_1^k = \|\boldsymbol{l}^k\| - l_0^k + \frac{1}{30 l_0^k}\left[2(\varepsilon_3^k)^2 + \varepsilon_3^k\varepsilon_4^k + 2(\varepsilon_4^k)^2 + 2(\varepsilon_5^k)^2 + \varepsilon_5^k\varepsilon_6^k + 2(\varepsilon_6^k)^2\right], \tag{2.4a}$$

$$\text{torsion}\quad :\quad \varepsilon_2^k = D_2^k = [(\boldsymbol{R}^p\boldsymbol{n}_{\bar{z}}, \boldsymbol{R}^q\boldsymbol{n}_{\bar{y}}) - (\boldsymbol{R}^p\boldsymbol{n}_{\bar{y}}, \boldsymbol{R}^q\boldsymbol{n}_{\bar{z}})]\,l_0^k/2\,, \tag{2.4b}$$

$$\text{bending}\quad :\quad \varepsilon_3^k = D_3^k = -(\boldsymbol{R}^p\boldsymbol{n}_{\bar{z}}, \boldsymbol{l}^k)\,, \tag{2.4c}$$

$$\varepsilon_4^k = D_4^k = (\boldsymbol{R}^q\boldsymbol{n}_{\bar{z}}, \boldsymbol{l}^k)\,, \tag{2.4d}$$

$$\varepsilon_5^k = D_5^k = (\boldsymbol{R}^p\boldsymbol{n}_{\bar{y}}, \boldsymbol{l}^k)\,, \tag{2.4e}$$

$$\varepsilon_6^k = D_6^k = -(\boldsymbol{R}^q\boldsymbol{n}_{\bar{y}}, \boldsymbol{l}^k)\,. \tag{2.4f}$$

Here, $\|\boldsymbol{l}^k\|$ and l_0^k represent the actual length and the reference length of the element; (,)

stands for the inner product of two vectors. The quadratic terms in the bending deformations in the expression for the elongation ε_1^k represent the longitudinal deformation associated with the deflection of the beam element. The deformation mode coordinates in (2.4) possess the proper invariance with respect to rigid body motions of the beam element. Since the expressions for the bending deformations are defined with respect to orthogonal triads oriented according to the element axis and the principle axes of its cross section, they have a clear physical meaning. If the deformations (ε_i^k) remain sufficiently small $(\varepsilon_i^k/l^k << 1)$, then in the elastic range they are linearly related to known beam quantities as normal force σ_1^k, twisting moment σ_2^k and bending moments σ_3^k, σ_4^k, σ_5^k, σ_6^k by the beam constitutive equations

$$\boldsymbol{\sigma}^k = \boldsymbol{S}^k \boldsymbol{\varepsilon}^k , \tag{2.5}$$

where $\boldsymbol{S}^k$ is a symmetric matrix containing the elastic constants. The components of $\boldsymbol{S}^k$ are calculated using third-order polynomial interpolations for the deformations of the element. The stiffness matrix is invariant under rigid body motions of the element and is the same matrix that occurs in linear finite element theory. For a prismatic beam element with the $\bar{y}$ and $\bar{z}$ axis in a cross-section along the principle axes, the elasticity coefficients of $\boldsymbol{S}^k$ are given by [12]:

$$\boldsymbol{S}^k = \begin{bmatrix} S_1^k & 0 & 0 & 0 & 0 & 0 \\ & S_2^k & 0 & 0 & 0 & 0 \\ & & 4S_3^k & -2S_3^k & 0 & 0 \\ & & \text{symm.} & 4S_3^k & 0 & 0 \\ & & & & 4S_4^k & -2S_4^k \\ & & & & & 4S_4^k \end{bmatrix},$$

where

$$S_1^k = \frac{E^k A^k}{l^k} , \qquad S_2^k = \frac{S_t^k}{(l^k)^3} , \qquad S_3^k = \frac{E^k I_{\bar{y}}^k}{(l^k)^3} , \qquad S_4^k = \frac{E^k I_{\bar{z}}^k}{(l^k)^3} . \tag{2.6}$$

Other relations between $\boldsymbol{\sigma}^k$ and $\boldsymbol{\varepsilon}^k$ are also possible for example describing viscoelastic behaviour of the element [6].

In addition to the physical deformations we must consider condition (2.3) to be imposed on the Euler parameters. For each orthogonal triad we introduce a deformation function of the so-called lambda element

$$e^k = D^k(\boldsymbol{\lambda}^k) = \boldsymbol{\lambda}^{kt}\boldsymbol{\lambda}^k - 1 . \tag{2.7}$$

Then the constrained condition for the Euler parameters is of similar form as the undeformability condition $(e^k = 0)$ for the λ-element.

2.2. The cylindrical hinge element

With this element, hereafter simply called hinge element, we are able to connect beam elements using a cylindrical hinge. As shown in Fig. 2 the hinge element has two nodes p and q located at the element axis. The configuration of the element is determined by two sets of

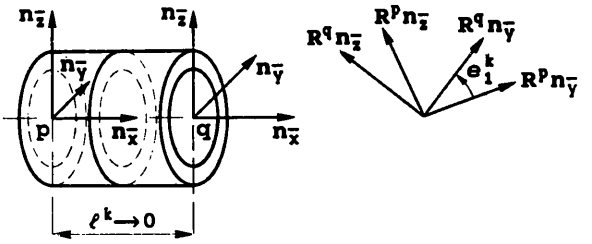

Fig. 2. Hinge element.

Euler parameters $(\lambda_i^p, \lambda_i^q)^k$ describing the angular orientation of orthogonal triads rigidly attached to each end-point. The vectors $n_{\bar{x}}$ of the hinge joints coincide with the hinge axis, the directions of the vectors $n_{\bar{y}}$ and $n_{\bar{z}}$ of both hinge nodes coincide initially.

With properly chosen deformation functions, it is possible to describe the relative rotation of the hinge nodes p and q. The hinge condition requires that the vectors $\boldsymbol{R}^p\boldsymbol{n}_{\bar{x}}$ and $\boldsymbol{R}^q\boldsymbol{n}_{\bar{x}}$ should be parallel for all arbitrary hinge rotations. As deformation functions for the hinge element we define the relative rotation about the hinge axis and two orthogonal bending deformations. The following expressions for the deformation functions are used:

$$\text{relative rotation:} \quad e_1^k = D_1^k = \text{ATAN2}[-(\boldsymbol{R}^p\boldsymbol{n}_{\bar{y}}, \boldsymbol{R}^q\boldsymbol{n}_{\bar{z}}), (\boldsymbol{R}^p\boldsymbol{n}_{\bar{y}}, \boldsymbol{R}^q\boldsymbol{n}_{\bar{y}})], \tag{2.8a}$$

$$\text{bending:} \quad \varepsilon_2^k = D_2^k = (\boldsymbol{R}^p\boldsymbol{n}_{\bar{y}}, \boldsymbol{R}^q\boldsymbol{n}_{\bar{x}}), \tag{2.8b}$$

$$\varepsilon_3^k = D_3^k = (\boldsymbol{R}^p\boldsymbol{n}_{\bar{z}}, \boldsymbol{R}^q\boldsymbol{n}_{\bar{x}}). \tag{2.8c}$$

The relative rotation e_1^k is obtained from the computer ATAN2 function. The value range of this function is defined by $-\pi < \text{ATAN2} \leq \pi$, so that with this function both a relative rotation $0 \leq \varphi \leq \pi$ and a relative rotation $-\pi < \varphi \leq 0$ of the hinge can be described. The two bending deformations describe the bending of the hinge pin. The hinge condition requires zero bending of the hinge pin, i.e., $\varepsilon_2^k = \varepsilon_3^k = 0$.

3. Kinematical analysis

A kinematic mechanism model can be built up with finite elements by letting them have nodal points in common. In this way, the configuration spaces of the individual elements can be regarded as subspaces of the mechanism configuration space X, that is

$$X = \sum_k X^k . \tag{3.1}$$

The element deformation spaces form together the space E of deformation mode coordinates for the entire mechanism. Since deformation mode coordinates (e_i^k) are only concerned with the element k, E is the direct sum of the spaces E^k, that is

$$E = \bigoplus_k E^k . \tag{3.2}$$

The deformation functions of the individual elements can be taken together in a continuity map for the entire mechanism; we write symbolically

$$D = \sum_k D^k : X \to E, \quad \text{or } e = D(x). \tag{3.3}$$

The continuity map in (3.3) constitutes the basic equations for the kinematic analysis. The kinematic constraints of a mechanism can be introduced in two ways:

(1) By prescribing some nodal coordinates (x_i). In particular the support coordinates have a prescribed constant value.

(2) By imposing conditions on the deformation mode coordinates (e_i). A frequently used mathematical model of a mechanism is the model in which the elastic deformation of the links is neglected. According to (3.3) the motion of the mechanism is then restricted to motions for which $\varepsilon = 0$.

An important concept in the kinematic and dynamic analysis of mechanisms is that of degrees of freedom (d.o.f.). The d.o.f. represent the least number of independent coordinates, called generalized coordinates, required to specify the configuration and deformation state of the mechanism. They may be chosen as absolute or as relative generalized coordinates. The latter are also used in the description of flexible elements. The spaces X and E can now be split into subspaces in accordance with the constraint conditions and the choice of the generalized coordinates. We have

$$X = X^o \oplus X^c \oplus X^m \quad \text{and} \quad E = E^o \oplus E^m \oplus E^c, \tag{3.4}$$

where the superscripts o, c and m denote the space of invariant, dependent and independent (generalized) coordinates respectively. The problem now formulated for the kinematic analysis is the determination of the nodal coordinates and deformation mode coordinates for given discrete values of the generalized coordinates (x_i^m, e_i^m). Hence determine the maps

$$F^x : X^m \times E^m \to X, \quad \text{or } x = F^x(x^m, e^m), \tag{3.5}$$

$$F^e : X^m \times E^m \to E, \quad \text{or } e = F^e(x^m, e^m). \tag{3.6}$$

The maps F^x and F^e are called the geometric transfer functions of the mechanism; they express the configuration and deformation state as explicit functions of the set of generalized coordinates. From a geometrical point of view the maps F^x and F^e characterize a time independent configuration manifold $M(X)$ and a deformation manifold $M(E)$ in the spaces X and E, respectively, see Fig. 3. The continuity map $D(x)$ in (3.3) may be viewed as a mapping between the two manifolds $M(X)$ and $M(E)$. The configuration and deformation state of the mechanism at any instant is represented by a point on the manifolds. The time history, as the mechanism evolves from state to state, is then represented by a connected set of points on the manifolds and we refer to these sets of points as the trajectories of the mechanism. At each point along the trajectories, there is a tangent vector that corresponds to the velocities of the mechanism. The tangent vectors are elements of the tangent spaces $TM(x)$ and $TM(e)$ at

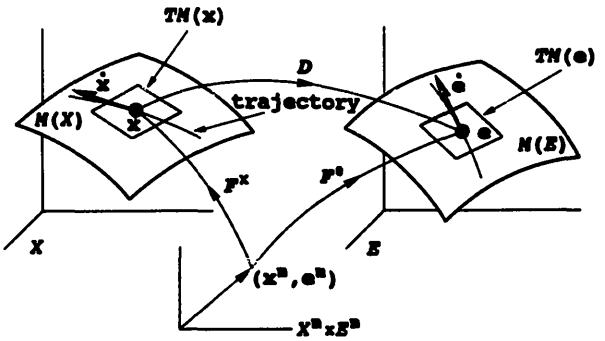

Fig. 3. Visualization of geometric transfer functions.

(x, e). The velocity vectors $\dot{x}$ and $\dot{e}$ at (x, e) can be calculated from (3.5) and (3.6) as

$$\dot{x} = \frac{\partial F^x}{\partial x^m}\,\dot{x}^m + \frac{\partial F^x}{\partial e^m}\,\dot{e}^m\,, \quad \text{or } \dot{x} = \mathrm{D}F^x \cdot (\dot{x}^m, \dot{e}^m)\,, \tag{3.7}$$

$$\dot{e} = \frac{\partial F^e}{\partial x^m}\,\dot{x}^m + \frac{\partial F^e}{\partial e^m}\,\dot{e}^m\,, \quad \text{or } \dot{e} = \mathrm{D}F^e \cdot (\dot{x}^m, \dot{e}^m)\,, \tag{3.8}$$

where $(\dot{})$ denotes differentiation with respect to time. The derivative maps $\mathrm{D}F^x$ and $\mathrm{D}F^e$ are called the first-order geometric transfer functions. From Fig. 3 we can deduce an algebraic relation between the functions F^x and F^e and the continuity equations $D(x)$:

$$F^e = D \circ F^x \quad \text{for all } (x^m, e^m)\,. \tag{3.9}$$

Due to the nonlinear character of the continuity equations the unknown geometric transfer functions F^x and F^e cannot be calculated directly from the equations in (3.9). It will be shown first that expressions for the first-order geometric transfer functions, can be obtained from the derivative map $\mathrm{D}D$. Differentiation of (3.9) yields with the chain rule

$$\mathrm{D}_i F^e = \mathrm{D}D(x) \cdot \mathrm{D}_i F^x\,, \tag{3.10}$$

where $\mathrm{D}_i F$ is the partial derivative of F with respect to its ith argument. The differentiation operator D working on $D(x)$ represents partial differentiation with respect to the nodal coordinates (x_i). The derivative map $\mathrm{D}D(x)$ is composed from the derivative maps $\mathrm{D}D^k$ of the individual elements and may be viewed as a linear mapping between the tangent spaces $TM(x)$ and $TM(e)$. In accordance with the coordinate splitting in (3.4), the system in (3.10) can be partitioned as

$$\begin{bmatrix} \mathrm{D}_i F^{eo} \\ \mathrm{D}_i F^{em} \\ \hline \mathrm{D}_i F^{ec} \end{bmatrix} = \left[\begin{array}{c|c|c} \mathrm{D}^o D^o & \mathrm{D}^c D^o & \mathrm{D}^m D^o \\ \hline \mathrm{D}^o D^m & \mathrm{D}^c D^m & \mathrm{D}^m D^m \\ \hline \mathrm{D}^o D^c & \mathrm{D}^c D^c & \mathrm{D}^m D^c \end{array}\right] \begin{bmatrix} \mathrm{D}_i F^{xo} \\ \mathrm{D}_i F^{xc} \\ \mathrm{D}_i F^{xm} \end{bmatrix}. \tag{3.11}$$

The superscripts o, c and m combined with the operator D represent partial differentiation with respect to the corresponding nodal coordinates (x_i^o), (x_i^c) and (x_i^m). The only unknowns

in this equation are the partial maps $\mathrm{D}\boldsymbol{F}^{xc}$ and $\mathrm{D}\boldsymbol{F}^{ec}$. For the other partial maps we have

$$\mathrm{D}\boldsymbol{F}^{eo} = \left[\frac{\partial \boldsymbol{e}^{o}}{\partial \boldsymbol{x}^{m}} \; \frac{\partial \boldsymbol{e}^{o}}{\partial \boldsymbol{e}^{m}}\right] = [\mathbf{0}, \mathbf{0}], \qquad \mathrm{D}\boldsymbol{F}^{em} = \left[\frac{\partial \boldsymbol{e}^{m}}{\partial \boldsymbol{x}^{m}} \; \frac{\partial \boldsymbol{e}^{m}}{\partial \boldsymbol{e}^{m}}\right] = [\mathbf{0}, \mathbf{I}], \tag{3.12}$$

$$\mathrm{D}\boldsymbol{F}^{xo} = \left[\frac{\partial \boldsymbol{x}^{o}}{\partial \boldsymbol{x}^{m}} \; \frac{\partial \boldsymbol{x}^{o}}{\partial \boldsymbol{e}^{m}}\right] = [\mathbf{0}, \mathbf{0}], \qquad \mathrm{D}\boldsymbol{F}^{xm} = \left[\frac{\partial \boldsymbol{x}^{m}}{\partial \boldsymbol{x}^{m}} \; \frac{\partial \boldsymbol{x}^{m}}{\partial \boldsymbol{e}^{m}}\right] = [\mathbf{I}, \mathbf{0}], \tag{3.13}$$

where **0** and **I** are the zero and identity matrix respectively. If the mechanism is not in a singular configuration, then the unknown first-order geometric transfer function $\mathrm{D}\boldsymbol{F}^{xc}$ can be calculated from (3.11) by

$$\mathrm{D}_i\boldsymbol{F}^{xc} = \begin{bmatrix}\mathrm{D}^{c}\boldsymbol{D}^{o}\\ \mathrm{D}^{c}\boldsymbol{D}^{m}\end{bmatrix}^{-1}\left\{\begin{bmatrix}\mathrm{D}_i\boldsymbol{F}^{eo}\\ \mathrm{D}_i\boldsymbol{F}^{em}\end{bmatrix} - \begin{bmatrix}\mathrm{D}^{m}\boldsymbol{D}^{o}\\ \mathrm{D}^{m}\boldsymbol{D}^{m}\end{bmatrix}[\mathrm{D}_i\boldsymbol{F}^{xm}]\right\} \tag{3.14}$$

and with (3.12) and (3.13) we obtain

$$\mathrm{D}\boldsymbol{F}^{xc} = \begin{bmatrix}\mathrm{D}^{c}\boldsymbol{D}^{o}\\ \mathrm{D}^{c}\boldsymbol{D}^{m}\end{bmatrix}^{-1}\begin{bmatrix}-\mathrm{D}^{m}\boldsymbol{D}^{o} & \mathbf{0}\\ -\mathrm{D}^{m}\boldsymbol{D}^{m} & \mathbf{I}\end{bmatrix}. \tag{3.15}$$

For the first-order geometric transfer function $\mathrm{D}\boldsymbol{F}^{ec}$, we obtain from (3.11)

$$\mathrm{D}_i\boldsymbol{F}^{ec} = \mathrm{D}^{c}\boldsymbol{D}^{c}\cdot\mathrm{D}_i\boldsymbol{F}^{xc} + \mathrm{D}^{m}\boldsymbol{D}^{c}\cdot\mathrm{D}_i\boldsymbol{F}^{xm}. \tag{3.16}$$

Expressions for the second-order geometric transfer functions can be obtained from the derivative map $\mathrm{D}\boldsymbol{D}$ in a similar way. Differentiation of (3.10) yields again, with the chain rule,

$$\mathrm{D}_{ij}\boldsymbol{F}^{e} = (\mathrm{D}^{2}\boldsymbol{D}\cdot\mathrm{D}_i\boldsymbol{F}^{x})\cdot\mathrm{D}_j\boldsymbol{F}^{x} + \mathrm{D}\boldsymbol{D}\cdot\mathrm{D}_{ij}\boldsymbol{F}^{x}, \tag{3.17}$$

where $\mathrm{D}^{2}\boldsymbol{D}$ is composed from the second partial derivatives $\mathrm{D}^{2}\boldsymbol{D}^{k}$ of the individual elements constituting the mechanism. In accordance with the coordinate splitting in (3.4), the system in (3.17) can be written in the form

$$\begin{bmatrix}\mathrm{D}_{ij}\boldsymbol{F}^{eo}\\ \mathrm{D}_{ij}\boldsymbol{F}^{em}\\ \mathrm{D}_{ij}\boldsymbol{F}^{ec}\end{bmatrix} = \begin{bmatrix}(\mathrm{D}^{2}\boldsymbol{D}^{o}\cdot\mathrm{D}_i\boldsymbol{F}^{x})\cdot\mathrm{D}_j\boldsymbol{F}^{x}\\ (\mathrm{D}^{2}\boldsymbol{D}^{m}\cdot\mathrm{D}_i\boldsymbol{F}^{x})\cdot\mathrm{D}_j\boldsymbol{F}^{x}\\ (\mathrm{D}^{2}\boldsymbol{D}^{c}\cdot\mathrm{D}_i\boldsymbol{F}^{x})\cdot\mathrm{D}_j\boldsymbol{F}^{x}\end{bmatrix} + \begin{bmatrix}\mathrm{D}^{o}\boldsymbol{D}^{c} & \mathrm{D}^{c}\boldsymbol{D}^{o} & \mathrm{D}^{m}\boldsymbol{D}^{o}\\ \mathrm{D}^{o}\boldsymbol{D}^{m} & \mathrm{D}^{c}\boldsymbol{D}^{m} & \mathrm{D}^{m}\boldsymbol{D}^{m}\\ \mathrm{D}^{o}\boldsymbol{D}^{c} & \mathrm{D}^{c}\boldsymbol{D}^{c} & \mathrm{D}^{m}\boldsymbol{D}^{c}\end{bmatrix}\begin{bmatrix}\mathrm{D}_{ij}\boldsymbol{F}^{xo}\\ \mathrm{D}_{ij}\boldsymbol{F}^{xc}\\ \mathrm{D}_{ij}\boldsymbol{F}^{xm}\end{bmatrix}, \tag{3.18}$$

where

$$\mathrm{D}_{ij}\boldsymbol{F}^{em} = \mathrm{D}_{ij}\boldsymbol{F}^{xm} = 0.$$

For the unknown second-order geometric transfer functions $\mathrm{D}^{2}\boldsymbol{F}^{xc}$ and $\mathrm{D}^{2}\boldsymbol{F}^{ec}$, we obtain

$$\mathrm{D}_{ij}\boldsymbol{F}^{xc} = -\begin{bmatrix}\mathrm{D}^{c}\boldsymbol{D}^{o}\\ \mathrm{D}^{c}\boldsymbol{D}^{m}\end{bmatrix}^{-1}\begin{bmatrix}(\mathrm{D}^{2}\boldsymbol{D}^{o}\cdot\mathrm{D}_i\boldsymbol{F}^{x})\cdot\mathrm{D}_j\boldsymbol{F}^{x}\\ (\mathrm{D}^{2}\boldsymbol{D}^{m}\cdot\mathrm{D}_i\boldsymbol{F}^{x})\cdot\mathrm{D}_j\boldsymbol{F}^{x}\end{bmatrix} \tag{3.19}$$

and

$$\mathrm{D}_{ij}\boldsymbol{F}^{ec} = (\mathrm{D}^{2}\boldsymbol{D}^{c}\cdot\mathrm{D}_i\boldsymbol{F}^{x})\cdot\mathrm{D}_j\boldsymbol{F}^{x} + \mathrm{D}^{c}\boldsymbol{D}^{c}\cdot\mathrm{D}_{ij}\boldsymbol{F}^{xc}. \tag{3.20}$$

For a mechanism with given kinematical dimensions, starting from a given configuration

(x_0, e_0) an initial second order prediction for an adjacent configuration (x_1, e_1) can be calculated taking into account the first and second-order terms of the Taylor series expansion of F^x and F^e at (x_0^m, e_0^m). We have

$$x_1 = x_0 + DF_0^x \cdot (\Delta x^m, \Delta e^m) + \tfrac{1}{2}(D^2 F_0^x \cdot (\Delta x^m, \Delta e^m)) \cdot (\Delta x^m, \Delta e^m), \tag{3.21}$$

$$e_1 = e_0 + DF_0^e \cdot (\Delta x^m, \Delta e^m) + \tfrac{1}{2}(D^2 F_0^e \cdot (\Delta x^m, \Delta e^m)) \cdot (\Delta x^m, \Delta e^m), \tag{3.22}$$

where

$$\Delta x^m = x_1^m - x_0^m \quad \text{and} \quad \Delta e^m = e_1^m - e_0^m .$$

A Newton–Raphson iteration process is then applied in order to guarantee that ultimately

$$D^m(x_1) = e_1^m \quad \text{and} \quad D^o(x_1) = 0 . \tag{3.23}$$

With the initial second order predictions in (3.21) and (3.22) a reliable convergence, even for comparatively large steps, is obtained.

4. Dynamical analysis

The basic laws of motion and the principle of virtual power are used to obtain the equations of motion. The inertia properties of the concentrated and distributed mass of the elements are described with the aid of mass matrices. Two formulations are employed in finite element theory.

4.1. Lumped formulation

For the determination of inertia forces with the help of lumped mass models it is sufficient to know the inertia forces of rigid bodies, acting at the end nodes of the element. Since Euler parameters are employed as rotational coordinates, the moment components of the force vectors should be converted to moment components associated with the time derivatives of the Euler parameters. Let us consider a lumped mass in the form of a rigid body attached to element node p described by the coordinates (x_i^p, λ_i^p). The seven coordinates define the location of the $(\bar{x}, \bar{y}, \bar{z})$ Cartesian coordinate system fixed in the body, relative to the global (inertial) coordinate axes (x, y, z), see Fig. 4. In the initial unrotated state of the body, the body-fixed coordinate system $(\bar{x}, \bar{y}, \bar{z})$ coincides with the global (inertial) coordinate system (x, y, z). The orientation of the body-fixed axes $(\bar{x}, \bar{y}, \bar{z})$ relative to the global coordinate system (x, y, z) is then determined by the rotation matrix R^p of (2.2). The velocity and angular velocity of the body at a given instant of time is determined by the vectors $\dot{x}^p$, representing the velocity of the origin of the body-fixed axes and the vector $\dot{\lambda}^p$ representing the time derivative of the Euler parameters. Let ω^p be the absolute angular velocity vector of the body, with components relative to the global coordinate system (x, y, z). The relationship between these components and the time derivative of the Euler parameters is determined by the transformation [11]

$$\omega^p = 2\Lambda^p \dot{\lambda}^p , \tag{4.1}$$

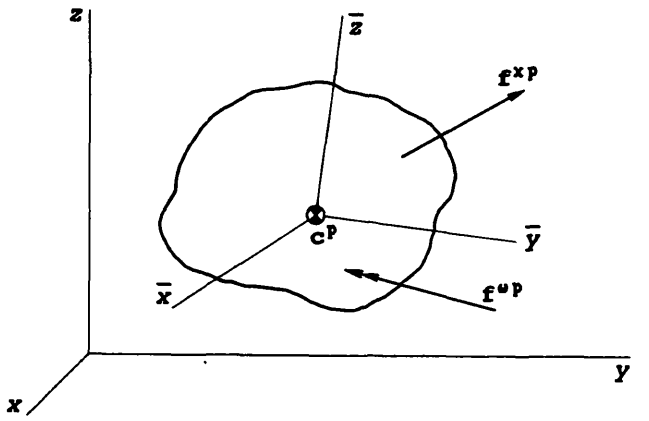

Fig. 4. Forces and torques acting on the rigid body.

where

$$\Lambda^p = \begin{bmatrix} -\lambda_1^p & \lambda_0^p & -\lambda_3^p & \lambda_2^p \\ -\lambda_2^p & \lambda_3^p & \lambda_0^p & -\lambda_1^p \\ -\lambda_3^p & -\lambda_2^p & \lambda_1^p & \lambda_0^p \end{bmatrix}. \tag{4.2}$$

The time derivatives of the Euler parameters must satisfy the constraint equation

$$2\lambda^{pt}\dot{\lambda}^p = 0, \tag{4.3}$$

which is obtained by differentiating (2.3) with respect to time. Let the origin of the body-fixed axes be located at the center of mass c^p, and let f^{xp} and $f^{\omega p}$ be the external force vector applied to the mass center c^p and the torque vector acting about that body's center of mass. The primitive forms of the dynamic equations of the body are those of Newton and Euler [13]:

$$f^{xp} = \frac{d}{dt}(M^p \dot{x}^p) \tag{4.4}$$

and

$$f^{\omega p} = \frac{d}{dt}(J^p \omega^p). \tag{4.5}$$

Here, M^p and J^p are the mass matrix and the rotational inertia matrix, the latter represent the rotational inertia tensor with respect to the mass center of the body. To apply (4.5) as a basis for the formalism of the rotational equations of motion of the body in terms of Euler parameters, we turn to the use of the principle of virtual power (Jourdain's principle). The principle states that for any motion the total power done by the forces of inertia and the actual forces is zero for all velocities associated with the virtual motion of the body. The power is defined by the scalar product $\langle\ ,\ \rangle$ of the velocity vector and a force vector which is the dual physical quantity representing the actual forces and the forces of inertia. For the rotational motion of the body the principle takes the form

$$\left\langle \left(f^{\omega p} - \frac{d}{dt}(J^p \omega^p) \right), \omega^p \right\rangle = 0, \tag{4.6}$$

for all $\boldsymbol{\omega}^p$, associated with the virtual motion of the body. By substituting (4.1) in the virtual power equation (4.6) we obtain the desired formulation in terms of Euler parameters. Since the time derivatives of the Euler parameters are dependent, by the constraint equation (4.3), the effect of this condition must be included in the virtual power equation. This can be done by using the Lagrange multiplier technique. With (4.1) and the constraint condition of (4.3) we then obtain

$$\left\langle \left(\boldsymbol{f}^{\omega p} - \frac{\mathrm{d}}{\mathrm{d}t} (2\boldsymbol{J}^p \boldsymbol{\Lambda}^p \dot{\boldsymbol{\lambda}}^p) \right), 2\boldsymbol{\Lambda}^p \dot{\boldsymbol{\lambda}}^p \right\rangle - \langle \sigma^{\lambda p}, 2\boldsymbol{\lambda}^{p\mathrm{t}} \dot{\boldsymbol{\lambda}}^p \rangle = 0 \quad \forall \dot{\boldsymbol{\lambda}}^p , \tag{4.7}$$

where $\sigma^{\lambda p}$ is the Lagrange multiplier associated with the constraint condition of (4.3). With the transpose of the transformations $\boldsymbol{\Lambda}^p$ and $\boldsymbol{\lambda}^{p\mathrm{t}}$ we obtain

$$\left\langle \left(\boldsymbol{f}^{\lambda p} - 2\boldsymbol{\Lambda}^{p\mathrm{t}} \frac{\mathrm{d}}{\mathrm{d}t} (2\boldsymbol{J}^p \boldsymbol{\Lambda}^p \dot{\boldsymbol{\lambda}}^p) - 2\boldsymbol{\lambda}^p \sigma^{\lambda p} \right), \dot{\boldsymbol{\lambda}}^p \right\rangle = 0 \quad \forall \dot{\boldsymbol{\lambda}}^p . \tag{4.8}$$

The components of the vector $\boldsymbol{f}^{\lambda p}$ are defined as

$$\boldsymbol{f}^{\lambda p} = 2\boldsymbol{\Lambda}^{p\mathrm{t}} \boldsymbol{f}^{\omega p} . \tag{4.9}$$

These are the four moment components associated with the time derivatives of the Euler parameters. In general the components of the inertia matrix $\boldsymbol{J}^p$ change as the body rotates. This dependence may be avoided by referring them to a set of axes fixed in the body. Therefore we introduce the following coordinate transformation

$$\boldsymbol{J}^p = \boldsymbol{R}^p \bar{\boldsymbol{J}}^p \boldsymbol{R}^{p\mathrm{t}} , \tag{4.10}$$

where $\bar{\boldsymbol{J}}^p$ denotes the inertia matrix with constant components referred to the body-fixed coordinate system $(\bar{x}, \bar{y}, \bar{z})$. $\boldsymbol{R}^p$ is the rotation matrix, defined in (2.2), which can be expressed as the result of two successive transformations as

$$\boldsymbol{R}^p = \boldsymbol{\Lambda}^p \bar{\boldsymbol{\Lambda}}^{p\mathrm{t}} , \tag{4.11}$$

where

$$\bar{\boldsymbol{\Lambda}}^p = \begin{bmatrix} -\lambda_1^p & \lambda_0^p & \lambda_3^p & -\lambda_2^p \\ -\lambda_2^p & -\lambda_3^p & \lambda_0^p & \lambda_1^p \\ -\lambda_3^p & \lambda_2^p & -\lambda_1^p & \lambda_0^p \end{bmatrix} . \tag{4.12}$$

Substituting (4.10) in (4.8) yields, with identity (4.11),

$$\left\langle \left(\boldsymbol{f}^{\lambda p} - 2\boldsymbol{\Lambda}^{p\mathrm{t}} \frac{\mathrm{d}}{\mathrm{d}t} (2\boldsymbol{\Lambda}^p \bar{\boldsymbol{\Lambda}}^{p\mathrm{t}} \bar{\boldsymbol{J}}^p \bar{\boldsymbol{\Lambda}}^p \boldsymbol{\Lambda}^{p\mathrm{t}} \boldsymbol{\Lambda}^p \dot{\boldsymbol{\lambda}}^p) - 2\boldsymbol{\lambda}^p \sigma^{\lambda p} \right), \dot{\boldsymbol{\lambda}}^p \right\rangle = 0 \quad \forall \dot{\boldsymbol{\lambda}}^p .$$

Carrying out the differentiation with respect to time by using the identities for the Euler parameters, yields [6]

$$\boldsymbol{f}^{\lambda p} = 4\bar{\boldsymbol{\Lambda}}^{p\mathrm{t}} \bar{\boldsymbol{J}}^p \bar{\boldsymbol{\Lambda}}^p \ddot{\boldsymbol{\lambda}}^p + 8\dot{\bar{\boldsymbol{\Lambda}}}^{p\mathrm{t}} \bar{\boldsymbol{J}}^p \bar{\boldsymbol{\Lambda}}^p \dot{\boldsymbol{\lambda}}^p + 2\boldsymbol{\lambda}^p \sigma^{\lambda p} . \tag{4.13}$$

These equations together with the constraint equation (4.3) describe the rotational motion of the body. Similar expressions are derived from Lagrange's Equations by Nikravesh [14]. The matrix $\bar{A}^{pt}\bar{J}^{p}\bar{A}^{p}$ is symmetric and positive definite. Naturally, it is configuration dependent, as shown by its dependence on λ.

The inertia forces associated with the lumped masses of the spatial beam element can now be characterized with the aid of the lumped mass matrix M_l^k and the rotational inertia tensor J_l^k. With (4.4) it follows that the lumped mass matrix of beam element k with nodes p and q can be written as

$$M_l^k = \begin{bmatrix} (M^x)_l^k & 0 \\ 0 & (M^\lambda)_l^k \end{bmatrix}, \tag{4.14}$$

where

$$(M^x)_l^k = \begin{bmatrix} M^p & 0 \\ 0 & M^q \end{bmatrix}^k \quad \text{and} \quad (M^\lambda)_l^k = 4\begin{bmatrix} \bar{A}^{pt}\bar{J}^{p}\bar{A}^{p} & 0 \\ 0 & \bar{A}^{qt}\bar{J}^{q}\bar{A}^{q} \end{bmatrix}^k.$$

The rate dependent inertia forces can be characterized by a quadratic velocity vector defined by

$$(J_l^k \cdot \dot{\lambda}^k)\cdot\dot{\lambda}^k = 8\begin{bmatrix} \dot{\bar{A}}^{p} & 0 \\ 0 & \dot{\bar{A}}^{q} \end{bmatrix}\begin{bmatrix} \bar{J}^{p} & 0 \\ 0 & \bar{J}^{q} \end{bmatrix}\begin{bmatrix} \dot{\lambda}^{p} \\ \dot{\lambda}^{q} \end{bmatrix}. \tag{4.15}$$

In case of a hinge element the lumped mass matrix becomes $M_l^k = (M^\lambda)_l^k$.

4.2. *Consistent mass formulation for the spatial beam element*

The derivation of the consistent mass formulation of the flexible beam element is based upon the elastic line concept. In order to account for the distributed inertia forces of the element, it is necessary to specify the elastic line configuration of the element in terms of the nodal coordinates (x_i^k, λ_i^k) and the flexible deformation mode coordinates (ε_i^k) such that the global position of every point on the elastic line is uniquely determined by these coordinates. At the boundary between the elements the position and orientation should be completely determined by the position and orientation of the corresponding node in order to guarantee structural continuity. The global position vector x^s of an arbitrary point s on the beam element in the undeflected state is specified in terms of the Cartesian nodal coordinates (x_i^k) as

$$x^s = \Phi x^k, \tag{4.16}$$

where

$$x^k = [x^{pt}, x^{qt}]^t.$$

The coefficient matrix Φ is defined by

$$\Phi = \left[\begin{array}{ccc|ccc} 1-\xi & 0 & 0 & \xi & 0 & 0 \\ 0 & 1-\xi & 0 & 0 & \xi & 0 \\ 0 & 0 & 1-\xi & 0 & 0 & \xi \end{array}\right], \tag{4.17}$$

with ξ being a normalized coordinate $(0 \leq \xi \leq 1)$, along the element axis measured from point p. Let $(\varepsilon_i^k,\ i = 3, 4, 5, 6)$ be the flexible deformation mode coordinates representing the

bending modes of the element k, defined in (2.4). Their geometric meaning is visualized in Fig. 5. Using cubic polynomial interpolations for the bending deformations, the global position vector r^s of point s in the deflected state of the element can be expressed as a vectorial sum of the vector x^s of the point s in the undeflected state and the elastic bending deformation with a displacement field expressed in terms of the flexible deformation mode coordinates (ε_i^k) as

$$r^s = x^s + \varepsilon_3^k R^p n_{\bar{z}}(\xi^3 - 2\xi^2 + \xi) + \varepsilon_4^k R^q n_{\bar{z}}(-\xi^3 + \xi^2) - \varepsilon_5^k R^p n_{\bar{y}}(\xi^3 - 2\xi^2 + \xi) - \varepsilon_6^k R^q n_{\bar{y}}(-\xi^3 + \xi^2), \tag{4.18}$$

where

$$n_{\bar{z}} = C^k n_z \quad \text{and} \quad n_{\bar{y}} = C^k n_y . \tag{4.19}$$

Here, C^k is an orthogonal matrix relating the principle element axes in the initial undeflected state with respect to the global (x, y, z) coordinate system. The polynomial equation (4.18) shows that the displacement field associated with the bending deformation of the beam element is described with respect to local coordinate systems that coincide with the orthogonal triads $(n_{\bar{x}}, n_{\bar{y}}, n_{\bar{z}})$ at the element nodes p and q. The interpolation functions satisfy differentiability requirements and with expression (4.18) the completeness and continuity requirements for the element are fulfilled. Let $\alpha(\xi)$ and $\beta(\xi)$ be polynomial vectors defined by

$$\alpha_z = n_z(\xi^3 - 2\xi^2 + \xi), \qquad \alpha_y = n_y(\xi^3 - 2\xi^2 + \xi) \tag{4.20a}$$

and

$$\beta_z = n_z(-\xi^3 + \xi^2), \qquad \beta_y = n_y(-\xi^3 + \xi^2). \tag{4.20b}$$

Substituting (4.16), (4.19) and (4.20) in (4.18) yields

$$r^s = [\Phi \mid R^p C^k \alpha_z, R^q C^k \beta_z, -R^p C^k \alpha_y, -R^q C^k \beta_y] \begin{bmatrix} x^k \\ \varepsilon^k \end{bmatrix}, \tag{4.21}$$

where

$$\varepsilon^k = [\varepsilon_3^k, \varepsilon_4^k, \varepsilon_5^k, \varepsilon_6^k]^t . \tag{4.22}$$

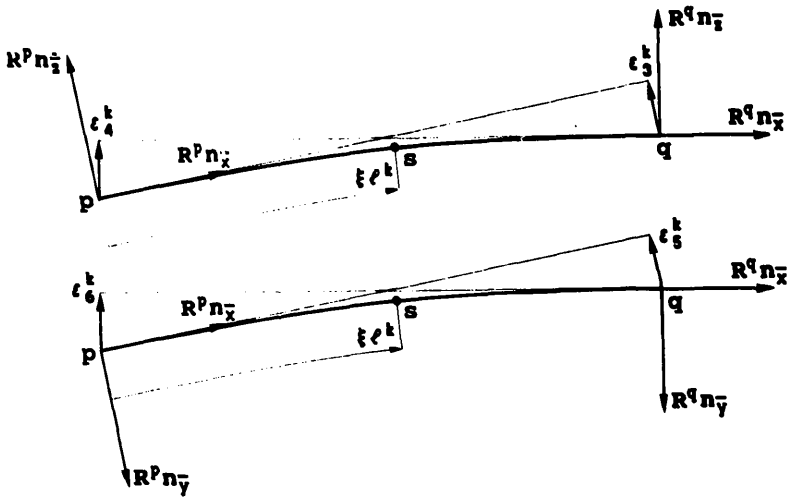

Fig. 5. Visualization of deformation modes representing the deflection of the spatial beam element.

To apply (4.21) as a basis for the consistent mass formalism of the element we turn to the use of the principle of virtual power. The virtual power of the distributed inertia forces, associated with the elastic line configuration of the beam element, can be expressed by the scalar product

$$-m^k l^k \int_0^1 \langle \dot{r}^s, \ddot{r}^s \rangle \, \mathrm{d}\xi \,, \tag{4.23}$$

where m^k is the mass density of the element per unit length and l^k is the length of the element. Evaluation of (4.23) leads to the general consistent mass formulation of the spatial beam element. Differentiating (4.21) with respect to time yields

$$\begin{aligned} \dot{r}^s = {} & [\Phi \,|\, R^p C^k \alpha_z, R^q C^k \beta_z, -R^p C^k \alpha_y, -R^q C^k \beta_y] \begin{bmatrix} \dot{x}^k \\ \dot{\varepsilon}^k \end{bmatrix} \\ & + [\dot{R}^p C^k \alpha_z, \dot{R}^q C^k \beta_z, -\dot{R}^p C^k \alpha_y, -\dot{R}^q C^k \beta_y] \varepsilon^k \,. \end{aligned} \tag{4.24}$$

It can be shown that the terms containing $\dot{R}^p$ and $\dot{R}^q$ can be written as

$$\dot{R}^p C^k \alpha_z = A_z \dot{\lambda}^p \,, \qquad \dot{R}^p C^k \alpha_y = A_y \dot{\lambda}^p \tag{4.25a}$$

and

$$\dot{R}^q C^k \beta_z = B_z \dot{\lambda}^q \,, \qquad \dot{R}^q C^k \beta_y = B_y \dot{\lambda}^q \,, \tag{4.25b}$$

where the matrices A_z and A_y are defined as

$$(A_{il})_z = R^p_{ij,l} C^k_{jm} (\alpha_m)_z \,, \qquad (A_{il})_y = R^p_{ij,l} C^k_{jm} (\alpha_m)_y$$

and B_z, B_y as

$$(B_{il})_z = R^q_{ij,l} C^k_{jm} (\beta_m)_z \,, \qquad (B_{il})_y = R^q_{ij,l} C^k_{jm} (\beta_m)_y \,.$$

In these expressions the index notation with the summation convention has been used. The components of $R_{ij,l}$ are partial derivatives of the rotation matrix R_{ij} with respect to λ_l. Substituting (4.25) in (4.24) yields

$$\dot{r}^s = [\Phi \,|\, \varepsilon_3^k A_z - \varepsilon_5^k A_y, \varepsilon_4^k B_z - \varepsilon_6^k B_y \,|\, R^p C^k \alpha_z, R^q C^k \beta_z, -R^p C^k \alpha_y, -R^q C^k \beta_y] \begin{bmatrix} \dot{x}^k \\ \dot{\lambda}^k \\ \dot{\varepsilon}^k \end{bmatrix}, \tag{4.26}$$

The acceleration vector of the infinitesimal volume at point s on the element is obtained by differentiating (4.26) with respect to time,

$$\begin{aligned} \ddot{r}^s = {} & [\Phi \,|\, \varepsilon_3^k A_z - \varepsilon_5^k A_y, \varepsilon_4^k B_z - \varepsilon_6^k B_y \,|\, R^p C^k \alpha_z, R^q C^k \beta_z, -R^p C^k \alpha_y, -R^q C^k \beta_y] \begin{bmatrix} \ddot{x}^k \\ \ddot{\lambda}^k \\ \ddot{\varepsilon}^k \end{bmatrix} \\ & + 2[\dot{\varepsilon}_3^k A_z - \dot{\varepsilon}_5^k A_y, \dot{\varepsilon}_4^k B_z - \dot{\varepsilon}_6^k B_y] \dot{\lambda}^k + [\varepsilon_3^k \dot{A}_z - \varepsilon_5^k \dot{A}_y, \varepsilon_4^k \dot{B}_z - \varepsilon_6^k \dot{B}_y] \dot{\lambda}^k \,. \end{aligned} \tag{4.27}$$

Substituting (4.26) and (4.27) in (4.23) and neglecting terms of $O(\varepsilon^2\ddot{\lambda})$, $O(\varepsilon\dot{\varepsilon}\dot{\lambda})$ and $O(\varepsilon^2\dot{\lambda}^2)$, one obtains

$$-m^k l^k \int_0^1 \langle \dot{r}^s, \ddot{r}^s \rangle \, d\xi = -[\dot{x}^{kt}, \dot{\lambda}^{kt}, \dot{\varepsilon}^{kt}] \left\{ \begin{bmatrix} (M^{xx})_c^k & (M^{x\lambda})_c^k & (M^{x\varepsilon})_c^k \\ (M^{\lambda x})_c^k & \mathbf{0} & (M^{\lambda\varepsilon})_c^k \\ (M^{\varepsilon x})_c^k & (M^{\varepsilon\lambda})_c^k & (M^{\varepsilon\varepsilon})_c^k \end{bmatrix} \begin{bmatrix} \ddot{x}^k \\ \ddot{\lambda}^k \\ \ddot{\varepsilon}^k \end{bmatrix} + \begin{bmatrix} ((J^x)_c^k \cdot \dot{\lambda}^k) \cdot \dot{\lambda}^k \\ \mathbf{0} \\ ((J^\varepsilon)_c^k \cdot \dot{\lambda}^k) \cdot \dot{\lambda}^k \end{bmatrix} + \begin{bmatrix} ((L^x)_c^k \cdot \dot{\varepsilon}^k) \cdot \dot{\lambda}^k \\ \mathbf{0} \\ ((L^\varepsilon)_c^k \cdot \dot{\varepsilon}^k) \cdot \dot{\lambda}^k \end{bmatrix} \right\}. \tag{4.28}$$

Here, M_c^k is the consistent mass matrix of the element k and $(J_c^k \cdot \dot{\lambda}^k) \cdot \dot{\lambda}^k$ and $(L_c^k \cdot \dot{\varepsilon}^k) \cdot \dot{\lambda}^k$ are quadratic velocity vectors representing the rate dependent inertia forces associated with the vectors $\dot{\varepsilon}^k$ and $\dot{\lambda}^k$. In Appendix A, expressions are presented for the partitioned mass matrices and for the rate dependent inertia vectors in (4.28). Significant further simplifications are possible by omitting terms linear in (ε_i^k), i.e., by omitting terms of $O(\varepsilon\ddot{x})$, $O(\varepsilon\ddot{\lambda})$, $O(\varepsilon\ddot{\varepsilon})$, $O(\varepsilon\dot{\lambda}^2)$ and $O(\dot{\varepsilon}\dot{\lambda})$ in (4.28). The associated simplified virtual power equation yields

$$-m^k l^k \int_0^1 \langle \dot{r}^s, \ddot{r}^s \rangle \, d\xi = -[\dot{x}^{kt}, \dot{\varepsilon}^{kt}] \begin{bmatrix} (M^{xx})_c^k & (M^{x\varepsilon})_c^k \\ (M^{\varepsilon x})_c^k & (M^{\varepsilon\varepsilon})_c^k \end{bmatrix} \begin{bmatrix} \ddot{x}^k \\ \ddot{\varepsilon}^k \end{bmatrix}. \tag{4.29}$$

These equations represent the reduced system of inertia forces of the element k. The matrices $(M^{x\varepsilon})_c^k$ and $(M^{\varepsilon x})_c^k$ represent the principal dynamic coupling between the gross motion and the elastic deformation of the element. It is shown in the Appendix that the matrices $(M^{x\lambda})_c^k$, $(M^{\varepsilon\lambda})_c^k$ and the components of $(J^x)_c^k$ and $(J^\varepsilon)_c^k$ in (4.28) depend linearly on the flexible deformation mode coordinates (ε_i^k). This implies that the dynamics of the spatial beam element, undergoing only a deformation along the length of the element, is completely determined by the translational mass matrix $(M^{xx})_c^k$, defined in (A1a). Substituting (4.17) in (A1a) yields after evaluation of the integrals

$$\begin{matrix} & \begin{bmatrix} x^p & y^p & z^p & x^q & y^q & z^q \end{bmatrix} \end{matrix}$$

$$(M^{xx})_c^k = \frac{m^k l^k}{6} \begin{bmatrix} 2 & 0 & 0 & 1 & 0 & 0 \\ & 2 & 0 & 0 & 1 & 0 \\ & & 2 & 0 & 0 & 1 \\ & \text{symm.} & & 2 & 0 & 0 \\ & & & & 2 & 0 \\ & & & & & 2 \end{bmatrix}. \tag{4.30}$$

This is the same mass matrix that occurs in linear finite element analysis representing the consistent mass matrix for a pin-joint bar element [7].

4.3. *Equations of motion*

In view of the different treatment of the translational and angular velocities in the derivation of the dynamic equations, it is useful to split the configuration space X of

mechanism nodal coordinates into subspaces according to

$$X = X^x \oplus X^\lambda , \qquad x \in X^x , \qquad \lambda \in X^\lambda , \tag{4.31}$$

where X^x is the space of Cartesian coordinates (x_i) and X^λ is the space of Euler parameters (λ_i). The corresponding geometric transfer functions are defined as

$$F^x : X^m \times E^m \to X^x , \quad x = F^x(x^m, e^m) , \tag{4.32a}$$

$$F^\lambda : X^m \times E^m \to X^\lambda , \quad \lambda = F^\lambda(x^m, e^m) . \tag{4.32b}$$

The velocity vectors $\dot{x}$ and $\dot{\lambda}$ can be calculated from these functions as

$$\dot{x} = DF^x \cdot (\dot{x}^m, \dot{e}^m) , \quad \dot{x} \in TM^x(x) , \tag{4.33a}$$

$$\dot{\lambda} = DF^\lambda \cdot (\dot{x}^m, \dot{e}^m) , \quad \dot{\lambda} \in TM^\lambda(x) . \tag{4.33b}$$

Let F^x be the space of externally applied nodal forces f^x and let F^λ be the space of externally applied torques f^λ, defined by (4.9). F^x and F^λ are dual with the tangent spaces $TM^x(x)$ and $TM^\lambda(x)$. The spaces F and $TM(x)$ are connected by the scalar product, representing the power. The loading state of each element consituting the mechanism is described by the stress vector $\sigma^k \in \Sigma^k$. The spaces Σ^k form together the space Σ of stress vectors for the entire mechanism, that is

$$\Sigma = \bigoplus_k \Sigma^k . \tag{4.34}$$

The space Σ is dual with the tangent space $TM(e)$. Note that in the Σ-space also the vector σ^λ, associated with the λ-elements is included. Let M be the mechanism mass matrix obtained by adding of the element matrices M_l^k and M_c^k defined in (4.14) and (A1), i.e.,

$$M = \sum_k (M_l^k + M_c^k) , \tag{4.35}$$

where the summation includes all elements. Furthermore, the inertia tensors J and L can be obtained in a similar way

$$J = \sum_k (J_l^k + J_c^k) \quad \text{and} \quad L = \sum_k L_c^k , \tag{4.36}$$

where J_l^k, J_c^k and L_c^k are defined in (4.15), (A2) and (A3), respectively. According to the principle of virtual power for the vectors of external forces and torques f^x, f^λ and the stress vector σ we then obtain

$$\left\langle \left(\begin{bmatrix} f^x \\ f^\lambda \\ -\sigma \end{bmatrix} - \begin{bmatrix} M^{xx} & M^{x\lambda} & M^{xe} \\ M^{\lambda x} & M^{\lambda\lambda} & M^{\lambda e} \\ M^{ex} & M^{e\lambda} & M^{ee} \end{bmatrix} \begin{bmatrix} \ddot{x} \\ \ddot{\lambda} \\ \ddot{e} \end{bmatrix} - \begin{bmatrix} (J^x \cdot \dot{\lambda}) \cdot \dot{\lambda} \\ (J^\lambda \cdot \dot{\lambda}) \cdot \dot{\lambda} \\ (J^e \cdot \dot{\lambda}) \cdot \dot{\lambda} \end{bmatrix} - \begin{bmatrix} (L^x \cdot \dot{\varepsilon}) \cdot \dot{\lambda} \\ 0 \\ (L^e \cdot \dot{\varepsilon}) \cdot \dot{\lambda} \end{bmatrix} \right), \begin{bmatrix} \dot{x} \\ \dot{\lambda} \\ \dot{e} \end{bmatrix} \right\rangle = 0 , \tag{4.37}$$

for all velocities $\dot{x}$, $\dot{\lambda}$ and $\dot{e}$ associated with the virtual motion of the mechanism which are defined by (4.33) and (3.8). From these equations we can calculate the accelerations $\ddot{x}$, $\ddot{\lambda}$ and $\ddot{\varepsilon}$ as functions of $(\dot{x}^m, \dot{e}^m)$ and $(\ddot{x}^m, \ddot{e}^m)$ by:

$$\ddot{x} = (D^2F^x \cdot (\dot{x}^m, \dot{e}^m)) \cdot (\dot{x}^m, \dot{e}^m) + DF^x \cdot (\ddot{x}^m, \ddot{e}^m), \tag{4.38a}$$

$$\ddot{\lambda} = (D^2F^\lambda \cdot (\dot{x}^m, \dot{e}^m)) \cdot (\dot{x}^m, \dot{e}^m) + DF^\lambda \cdot (\ddot{x}^m, \ddot{e}^m), \tag{4.38b}$$

$$\ddot{\varepsilon} = (D^2F^\varepsilon \cdot (\dot{x}^m, \dot{e}^m)) \cdot (\dot{x}^m, \dot{e}^m) + DF^\varepsilon \cdot (\ddot{x}^m, \ddot{e}^m). \tag{4.39}$$

Substituting (4.33), (3.8) and (4.38), (4.39) in the virtual power equation (4.37) yields with the dual transformations DF^{xt}, $DF^{\lambda t}$ and DF^{et}:

$$[DF^{xt}, DF^{\lambda t}, DF^{\varepsilon t}] \begin{bmatrix} M^{xx} & M^{x\lambda} & M^{x\varepsilon} \\ M^{\lambda x} & M^{\lambda\lambda} & M^{\lambda\varepsilon} \\ M^{\varepsilon x} & M^{\varepsilon\lambda} & M^{\varepsilon\varepsilon} \end{bmatrix} \begin{bmatrix} DF^x \\ DF^\lambda \\ DF^\varepsilon \end{bmatrix} \begin{bmatrix} \ddot{x}^m \\ \ddot{e}^m \end{bmatrix}$$

$$= [DF^{xt}, DF^{\lambda t}, DF^{et}] \begin{bmatrix} f^x - f^x_{in} \\ f^\lambda - f^\lambda_{in} \\ -\sigma - \sigma_{in} \end{bmatrix}, \tag{4.40}$$

where

$$\begin{bmatrix} f^x_{in} \\ f^\lambda_{in} \\ \sigma_{in} \end{bmatrix} = \begin{bmatrix} (J^x \cdot \dot{\lambda}) \cdot \dot{\lambda} \\ (J^\lambda \cdot \dot{\lambda}) \cdot \dot{\lambda} \\ (J^\varepsilon \cdot \dot{\lambda}) \cdot \dot{\lambda} \end{bmatrix} + \begin{bmatrix} (L^x \cdot \dot{\varepsilon}) \cdot \dot{\lambda} \\ 0 \\ (L^\varepsilon \cdot \dot{\varepsilon}) \cdot \dot{\lambda} \end{bmatrix}$$

$$+ \begin{bmatrix} M^{xx} & M^{x\lambda} & M^{x\varepsilon} \\ M^{\lambda x} & M^{\lambda\lambda} & M^{\lambda\varepsilon} \\ M^{\varepsilon x} & M^{\varepsilon\lambda} & M^{\varepsilon\varepsilon} \end{bmatrix} \begin{bmatrix} (D^2F^x \cdot (\dot{x}^m, \dot{e}^m)) \cdot (\dot{x}^m, \dot{e}^m) \\ (D^2F^\lambda \cdot (\dot{x}^m, \dot{e}^m)) \cdot (\dot{x}^m, \dot{e}^m) \\ (D^2F^\varepsilon \cdot (\dot{x}^m, \dot{e}^m)) \cdot (\dot{x}^m, \dot{e}^m) \end{bmatrix}. \tag{4.41}$$

With the notation $[DF^t] = [DF^{xt}, DF^{\lambda t}, DF^{et}]$, the equations in (4.40) can be written as

$$[DF^t M DF] \begin{bmatrix} \ddot{x}^m \\ \ddot{e}^m \end{bmatrix} = [DF^t] \begin{bmatrix} f - f_{in} \\ -\sigma - \sigma_{in} \end{bmatrix}, \tag{4.42}$$

where $[DF^t M DF]$ is the system mass matrix of the mechanism. These are the equations of motion for the mechanism in their final form. They describe the general case of coupled rigid link motion and small elastic deformation. The force vector contains the nodal forces f applied to the mechanism nodes, but also the stress vector σ. The stresses of the flexible elements are characterized by Hooke's law defined in (2.5). In case of generalized coordinates (e_i^m) associated with large relative displacements and rotations, constitutive equations describing the behaviour of built-in driving actuators can be added to the system of equations. In this way it is possible to study the dynamics of active spatial mechanisms such as manipulators and robot mechanisms [8]. The equations of motion are integrated numerically for the independent generalized coordinates by a predictor/corrector algorithm with variable order and stepsize [15].

5. Some numerical examples

In order to demonstrate the capabilities of the analysis method and to investigate the effects of including geometric nonlinearities on the dynamic response of flexible link mechanisms, two examples are presented in this section, namely a spatial slider crank mechanism with flexible connecting rod and a rotating shaft passing through the major critical speed.

5.1. *Spatial slider crank mechanism*

The slider crank mechanism, shown in Fig. 6 consists of a rigid crank shaft OA of length $l_c = 0.15$ m, a flexible connecting rod AB of length $l_r = 0.3$ m and a slider block at B with a mass equal to half the mass of the connecting rod. The crank axis is rotated over an angle α about the global y-axis. The universal joint between the crank and the connecting rod is modelled by two hinge elements. The connecting rod and sliding block are connected by a spherical joint. The sliding block moves along the x-axis. The crank is driven with a constant angular speed $\Omega = 150$ rad/s. The connecting rod has a uniform circular cross section with a diameter of 0.006 m and is made of steel, having a density of 7.87×10^3 kg/m^3 and an elasticity modulus of 0.2×10^{12} N/m^2. The initial configuration of the slider crank is shown in Fig. 6b. The elastic connecting rod is assumed initially straight and its end conditions correspond to simple supports with a lowest bending frequency of 832.5 rad/s. Longitudinal and torsional deformations of the connecting rod due to the normal forces and the twisting moments are suppressed. Furthermore the torsional inertia of the connecting rod is neglected. The connecting rod is modelled using linear and nonlinear beam elements, depending on whether the geometric nonlinearities due to the quadratic terms in the bending deformations in the expressions for the longitudinal deformation ε_1^k are neglected or not. The dimensionless deflection of the midpoint of the connecting rod, measured perpendicularly to a straight line connecting points A and B, is calculated and represented by the components v_{xy}/l_r and v_{xz}/l_r being the projections of the deflection vector v/l_r on the xy-plane and on the xz-plane, see

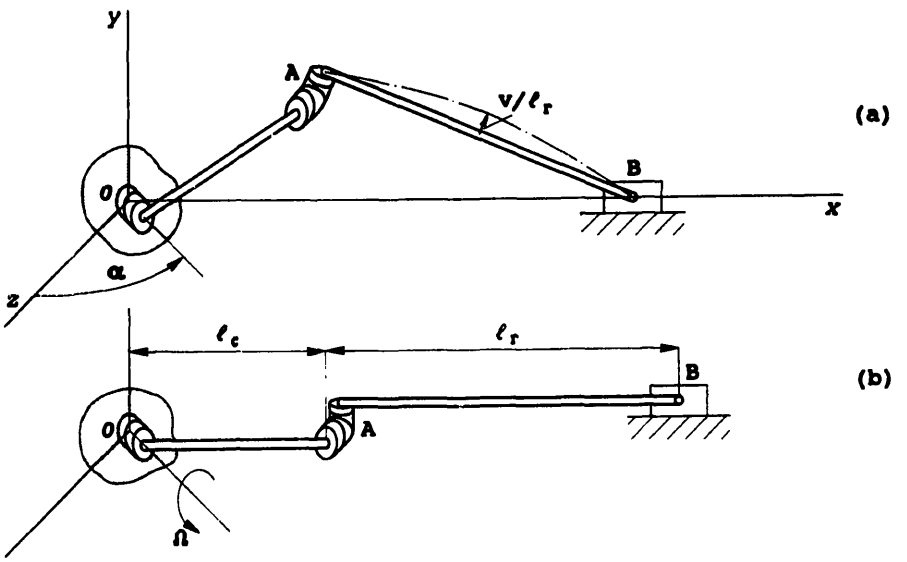

Fig. 6. (a) Spatial slider crank mechanism with flexible connecting rod. (b) Initial configuration of the slider crank.

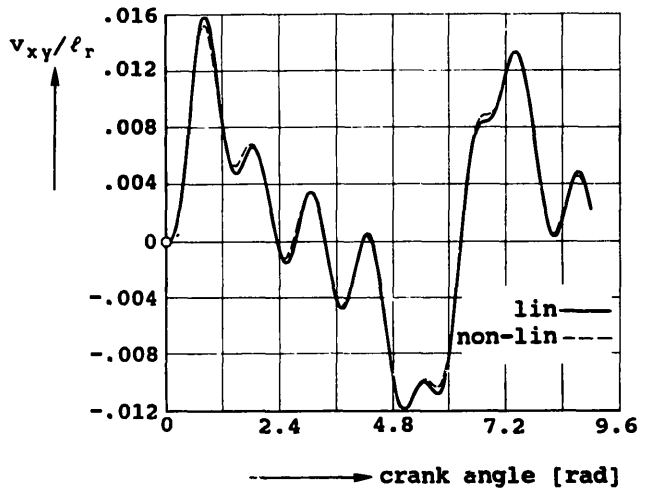

Fig. 7. Linear and nonlinear solutions for the planar mechanism ($\alpha = 0$, $v_{xz} \doteq 0$).

Fig. 6. The analysis is done for both the planar mechanism ($\alpha = 0$) and the spatial mechanism ($\alpha = \pi/4$), where the connecting rod is divided in two equal beam elements. Figure 7 shows a comparison between the linear and nonlinear solutions of the planar mechanism. It can be observed that the geometric nonlinearities have no significant effects on the behaviour of the solution. Very good agreement has been obtained between the linear response and a response obtained with the general purpose computer program DADS-3D (Dynamic analysis and design systems [16], [17]). The agreement was so good that the difference between the solutions is not visible when v_{xy}/l_r is plotted. Figure 8 shows a comparison between the nonlinear response and a similar nonlinear, two elements solution presented by Bahr and Shabana [18]. Figure 9 shows the nonlinear responses v_{xy}/l_r and v_{xz}/l_r of the spatial mechanism. In the dynamic simulations of the planar and the spatial slider crank mechanism, the inertia terms of $\mathcal{O}(\varepsilon)$ in the consistent mass formalism of the connecting rod did not significantly alter the flexible dynamic response of the connecting rod. However, these terms

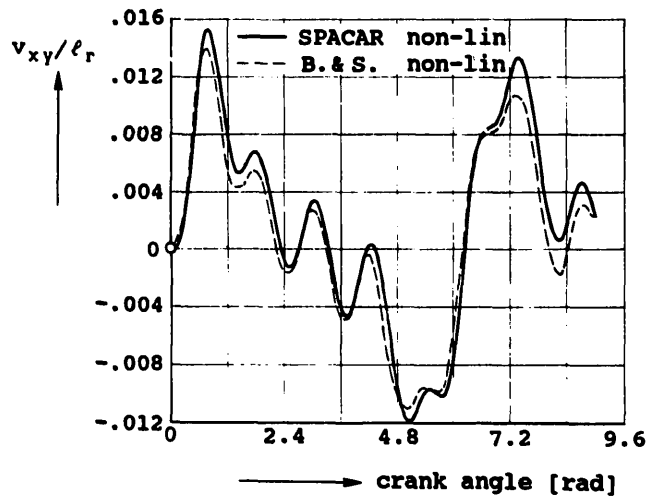

Fig. 8. Comparison between nonlinear solutions of SPACAR and Bahr and Shabana [18].

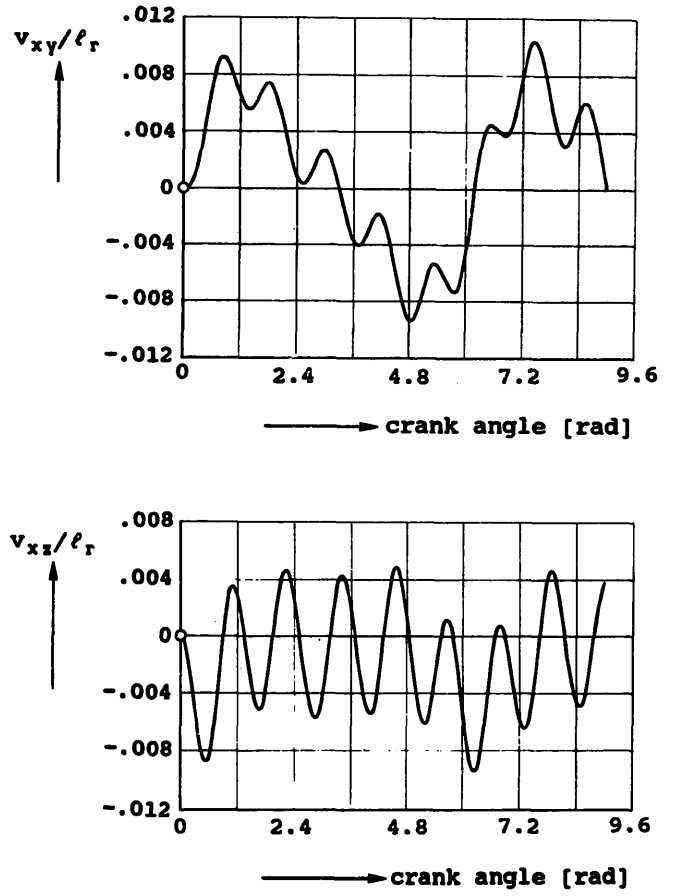

Fig. 9. Deflection components v_{xy}/l_r and v_{xz}/l_r of spatial slider crank mechanism ($\alpha = \pi/4$).

are of great importance when beam elements are used to model high-speed rotating shafts. This is illustrated in the next example.

5.2. *Transient vibrations of a rotating shaft passing through the major critical speed*

Figure 10 shows the nonlinear transient vibration of a simply supported shaft with symmetrical cross-section passing through the major critical speed with a constant angular acceleration $\dot{\Omega} = 1\,\text{rad/s}^2$. The shaft has a length $l = 0.3\,\text{m}$, a uniform circular cross section with a diameter of 0.006 m and is made of steel, having a density of $7.87 \times 10^3\,\text{kg/m}^3$ and an elasticity modulus of $0.2 \times 10^{12}\,\text{N/m}^2$. The internal damping of the shaft is modelled by a viscous damping coefficient of $1.27 \times 10^6\,\text{Ns/m}^2$. The simulation is performed for the case where the shaft is divided in two equal beam elements; the initial deflection v/l at the midpoint of the shaft is 0.006.

The responses demonstrate the remarkable destabilizing effect of the internal damping at speeds beyond the critical speeds. The effect of so-called rotary damping imposes an upper limit to the shaft speed above which the motion is always unstable. The limiting speed coincides with the major critical speed ω_c of the shaft system, in this example $\omega_c = 8.325 \times 10^2\,\text{rad/s}$.

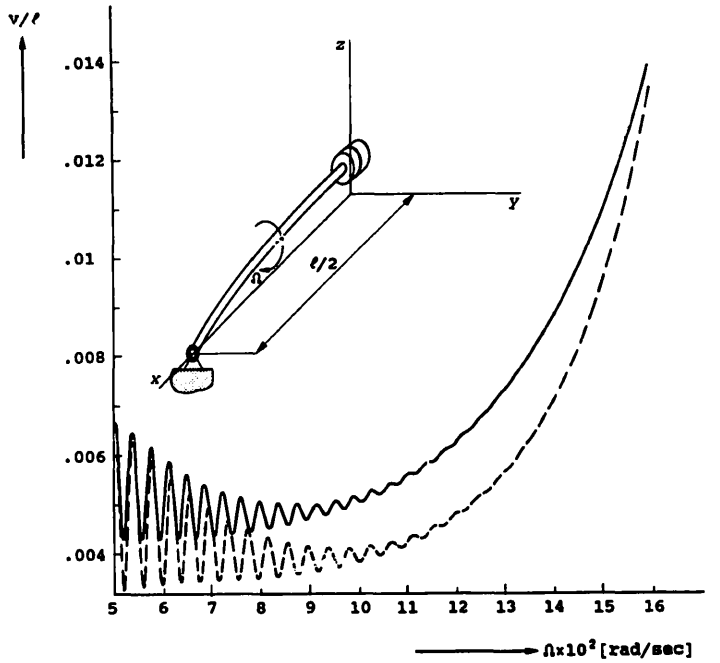

Fig. 10. Deflection v/l at the midpoint of a simply supported shaft passing through the major critical speed. —— with terms $O(\varepsilon)$, ---- without terms $O(\varepsilon)$.

6. Conclusions

The proposed finite element formulation has proved to be particularly useful for modelling of mechanisms with highly flexible links. In the formulation separate rigid body displacements and actual deformations are specified in the description of the current state of a finite element. This method simplified conceptually the nonlinear analysis involving large displacements and small (elastic) deformations.

For the elements presented, one can easily define by inspection a complete set of deformation modes. The ease by which the deformability can be handled leads to interesting possibilities of modelling joint elements like sliders and hinges. In the computer program SPACAR full advantage is taken of these possibilities.

Appendix A. Consistent mass matrices for the beam element

The mass matrices $(M^{xx})_c^k$, $(M^{x\lambda})_c^k$, $(M^{x\varepsilon})_c^k$, $(M^{\varepsilon\lambda})_c^k$ and $(M^{\varepsilon\varepsilon})_c^k$ in (4.28) are given by

$$(M^{xx})_c^k = m^k l^k \int_0^1 [\Phi^t \Phi]\, d\xi\,, \tag{A1a}$$

$$(M^{x\lambda})_c^k = (M^{\lambda x})_c^{kt} = m^k l^k \int_0^1 [\varepsilon_3^k \Phi^t A_z - \varepsilon_5^k \Phi^t A_y \mid \varepsilon_4^k \Phi^t B_z - \varepsilon_6^k \Phi^t B_y]\, d\xi\,, \tag{A1b}$$

$$(M^{x\varepsilon})_c^k = (M^{\varepsilon x})_c^{kt} = m^k l^k \int_0^1 [\Phi^t R^p C^k \alpha_z, \Phi^t R^q C^k \beta_z, -\Phi^t R^p C^k \alpha_y, -\Phi^t R^q C^k \beta_y]\, d\xi\,, \tag{A1c}$$

$$(M^{\varepsilon\lambda})_c^k = (M^{\lambda\varepsilon})_c^{kt} = m^k l^k \int_0^1 \begin{bmatrix} \alpha_z^t C^{kt} R^{pt} \\ \beta_z^t C^{kt} R^{qt} \\ -\alpha_y^t C^{kt} R^{pt} \\ -\beta_y^t C^{kt} R^{qt} \end{bmatrix} [\varepsilon_3^k A_z - \varepsilon_5^k A_y, \varepsilon_4^k B_z - \varepsilon_6^k B_y]\, d\xi\,, \tag{A1d}$$

$$(M^{\varepsilon\varepsilon})_c^k = m^k l^k \int_0^1 \begin{bmatrix} \alpha_z^t C^{kt} R^{pt} \\ \beta_z^t C^{kt} R^{qt} \\ -\alpha_y^t C^{kt} R^{pt} \\ -\beta_y^t C^{kt} R^{qt} \end{bmatrix} [R^p C^k \alpha_z, R^q C^k \beta_z, -R^p C^k \alpha_y, -R^q C^k \beta_y]\, d\xi\,. \tag{A1e}$$

The quadratic velocity vectors $((J^x)_c^k \cdot \dot{\lambda}^k) \cdot \dot{\lambda}^k$ and $((J^\varepsilon)_c^k \cdot \dot{\lambda}^k) \cdot \dot{\lambda}^k$ representing the rate dependent inertial forces in (4.28), associated with the time derivatives of the Euler parameters are given by

$$(J^x)_c^k \cdot \dot{\lambda}^k) \cdot \dot{\lambda}^k = m^k l^k \int_0^1 [\varepsilon_3^k \Phi^t \dot{A}_z - \varepsilon_5^k \Phi^t \dot{A}_y, \varepsilon_4^k \Phi^t \dot{B}_z - \varepsilon_6^k \Phi^t \dot{B}_y] \dot{\lambda}^k\, d\xi\,, \tag{A2a}$$

$$((J^\varepsilon)_c^k \cdot \dot{\lambda}^k) \cdot \dot{\lambda}^k = m^k l^k \int_0^1 \begin{bmatrix} \alpha_z^t C^{kt} R^{pt} \\ \beta_z^t C^{kt} R^{qt} \\ -\alpha_y^t C^{kt} R^{pt} \\ -\beta_y^t C^{kt} R^{qt} \end{bmatrix} [\varepsilon_3^k \dot{A}_z - \varepsilon_5^k \dot{A}_y, \varepsilon_4^k \dot{B}_z - \varepsilon_6^k \dot{B}_y] \dot{\lambda}^k\, d\xi\,. \tag{A2b}$$

Finally, the rate dependent inertia vectors $((L^x)_c^k \cdot \dot{\varepsilon}^k) \cdot \dot{\lambda}^k$ and $((L^\varepsilon)_c^k \cdot \dot{\varepsilon}^k) \cdot \dot{\lambda}^k$ in (4.28) are given by

$$((L^x)_c^k \cdot \dot{\varepsilon}^k) \cdot \dot{\lambda}^k = 2m^k l^k \int_0^1 [\dot{\varepsilon}_3^k \Phi^t A_z - \dot{\varepsilon}_5^k \Phi^t A_y, \dot{\varepsilon}_4^k \Phi^t B_z - \dot{\varepsilon}_6^k \Phi^t B_y] \dot{\lambda}^k\, d\xi\,, \tag{A3a}$$

$$((L^\varepsilon)_c^k \cdot \dot{\varepsilon}^k) \cdot \dot{\lambda}^k = 2m^k l^k \int_0^1 \begin{bmatrix} \alpha_z^t C^{kt} R^{pt} \\ \beta_z^t C^{kt} R^{qt} \\ -\alpha_y^t C^{kt} R^{pt} \\ -\beta_y^t C^{kt} R^{qt} \end{bmatrix} [\dot{\varepsilon}_3^k A_z - \dot{\varepsilon}_5^k A_y, \dot{\varepsilon}_4^k B_z - \dot{\varepsilon}_6^k B_y] \dot{\lambda}^k\, d\xi\,. \tag{A3b}$$

For a detailed evaluation of the inertial terms the reader is referred to [6].

References

[1] J.H. Argyris, Continua and discontinua, Proc. Conf. Matrix Methods in Structural Mechanics (Wright–Patterson A.F.B., Ohio, 1965).
[2] J.F. Besseling, The complete analogy between the matrix equations and the continuous field equations of structural analysis, Internat. Symp. Analogue and Digital Techniques Applied to Aeronautics, Liege, Belgium, 1963.
[3] J. Robinson, Integrated Theory of Finite Element Methods (Wiley, New York, 1973).
[4] K. van der Werff, Kinematic and dynamic analysis of mechanisms, a finite element approach, Doctors Thesis, Delft University of Technology, 1977.
[5] K. van der Werff and J.B. Jonker, Dynamics of flexible mechanisms, in: E.J. Haug, Ed., Computer aided analysis and optimization of mechanical system dynamics (Springer, Berlin, 1984) 381–400.
[6] J.B. Jonker, A finite element dynamic analysis of flexible spatial mechanisms and manipulators, Doctors Thesis, Delft University of Technology, Faculty of Mechanical Engineering, 1988.
[7] J.S. Przemieniecki, Theory of Matrix Structural Analysis (McGraw-Hill, New York, 1968).
[8] J.B. Jonker, Dynamics of active mechanisms with flexible links, Proc. IUTAM/IFToMM Symposium on Dynamics of Multibody Systems, Udine, Italy (1985) 103–118.
[9] W. Schiehlen, Technische Dynamik (Teubner, Stuttgart, 1985).
[10] J.B. Jonker and J.P. Meijard, SPACAR–program system for dynamic analysis of flexible spatial mechanisms and manipulators, in: W. Schiehlen, ed., Multibody System Handbook (Springer, Berlin, 1989).
[11] J. Wittenburg, Dynamics of Systems of Rigid Bodies (Teubner, Stuttgart, 1977).
[12] J.F. Besseling, Nonlinear theory for elastic beams and rods and its finite element representation, Comput. Methods Appl. Mech. Engrg. 31 (1982) 205–220.
[13] D.T. Greenwood, Principles of Dynamics (Prentice-Hall, Englewood Cliffs, NY, 1965).
[14] P.E. Nikravesh and I.S. Chung, Application of Euler parameters to the dynamic analysis of three-dimensional constrained mechanical systems, J. Mech. Design 104 (1982) 785–791.
[15] L.F. Shampine and M.K. Gordon, Computer Solution of Ordinary Differential Equations, The Initial Value Problem (W.J. Freeman, San Francisco, CA, 1975).
[16] W.S. Yoo and E.J. Haug, Dynamics of articulated structures, Part I: Theory, J. of Structural Mech. 14 (1986) 105–126.
[17] W.P. Koppens, The dynamics of systems of deformable bodies, Doctors Thesis, Eindhoven University of Technology, Faculty of Mechanical Engineering, 1989.
[18] E.M. Bahr and A.A. Shabana, Geometrically nonlinear analysis of multibody systems, Comput. & Structures 23 (6) (1986) 739–751.